The structure of the dynactin complex and its interaction with dynein

Linas Urnavicius[#1], **Kai Zhang**[#1], **Aristides G. Diamant**[#1], **Carina Motz**[1], **Max A. Schlager**[1], **Minmin Yu**[1], **Nisha A. Patel**[2], **Carol V. Robinson**[2], and **Andrew P. Carter**[1,†]

[1]Medical Research Council Laboratory of Molecular Biology, Division of Structural Studies, Francis Crick Avenue, Cambridge, CB2 0QH, UK

[2]Department of Chemistry, Physical and Theoretical Chemistry Laboratory, University of Oxford, Oxford OX1 3QZ, UK

[#] These authors contributed equally to this work.

Abstract

Dynactin is an essential cofactor for the microtubule motor cytoplasmic dynein-1. We report the structure of the 23 subunit dynactin complex by cryo-electron microscopy to 4.0Å. Our reconstruction reveals how dynactin is built around a filament containing eight copies of the actin related protein Arp1 and one of β-actin. Capped at each end by distinct protein complexes, the length of the filament is defined by elongated peptides that emerge from the α-helical shoulder domain. A further 8.2Å structure of the complex between dynein, dynactin and the motility inducing cargo adaptor Bicaudal-D2 shows how the translational symmetry of the dynein tail matches that of the dynactin filament. The Bicaudal-D2 coiled coil runs between dynein and dynactin to stabilize the mutually dependent interactions between all three components.

Dynactin works with the cytoplasmic dynein-1 motor (dynein) to transport cargos along the microtubule cytoskeleton (1-3). They maintain the cell's spatial organization, return components from the cell's periphery and assist with cellular division (4). Mutations in either complex cause neurodegeneration (5) and both can be co-opted by viruses that travel to the nucleus (6). Dynein and dynactin are similar in size and complexity. Dynein contains two copies of 6 different proteins and has a mass of 1.4 MDa. Dynactin, at about 1.0 MDa, contains more than 20 subunits, corresponding to 12 different proteins. Dynactin is built around a filament of actin related protein 1 (Arp1). In analogy to actin, the filament has a barbed and a pointed end; each capped by a different protein complex. On top sits the shoulder domain (7) from which emerges a long projection, corresponding to dynactin's largest subunit p150^Glued (DCTN1) (8).

Despite the presence of a dynein binding site in p150^Glued (9-11), purified dynein and dynactin only form a stable complex in the presence of the cargo adaptor Bicaudal D2

(BICD2) (12-14), a coiled coil protein associated with transport of vesicles, mRNAs and nuclei (15). This interaction activates dynein and converts it into a highly processive motor (13, 14).

Current models for dynactin's architecture (7, 16, 17) and its interaction with dynein (13, 14) come from low resolution negative stain and platinum shadowing electron microscopy. A number of questions remain. What makes the filament in dynactin short and defined, when purified Arp1 filaments vary in length (18)? How does dynein bind to dynactin and why does the interaction require BICD2 (12-14)? Why does dynactin, the co-factor for a microtubule motor, contain an actin-related filament? To address these questions we took advantage of recent advances in cryo-electron microscopy (cryo-EM) (19) to improve our structural understanding of dynactin.

Dynactin structure determination

Dynactin is a challenging target for cryo-EM (17). Its extreme preferred orientation on EM grids makes it hard to obtain the broad distribution of views required for a 3D reconstruction. Furthermore dynactin's thin elongated shape limits its contrast, making it difficult to assign views accurately. We overcame these hurdles (20) to determine cryo-EM maps of native dynactin purified from pig brain (fig. S1); initially at 6.3Å (table S1:Dynactin-1) and subsequently at 3.9Å overall and 3.5Å in the dynactin filament (table S1:Dynactin-2,3,4 Fig. 1A,B, fig. S2 and movies S1-2). We used both maps to build a model of dynactin (Fig. 1C and table S2). The filament and pointed end capping protein Arp11 were built de-novo and refined (table S3). Homology models of the barbed end capping protein CapZαβ (21), and the pointed end proteins p25 (DCTN5) and p27 (DCTN6) (22) were fitted into density. The pointed end protein p62 and the shoulder, which contains p150^{Glued} (DCTN1), p50 (dynamitin or DCTN2) and p24 (DCTN3), were built as backbone models (Fig. 1D).

The dynactin filament contains eight Arp-1 subunits and one β-actin

The dynactin filament is nine subunits long and consists of two protofilaments that wrap around each other (Fig. 1A,C): five subunits (A,C,E,G,I) in the top protofilament and four (B,D,F,H) in the bottom. The presence of β-actin in the filament is controversial (7, 23). Our cryo-EM map was of sufficient quality (fig. S3A) to show that subunit-H is β-actin (β-actin-H), while the others are Arp1 (Arp1-A to Arp1-I). We confirmed the presence of Arp1 and β-actin at an 8:1 ratio by mass spectrometry-based label-free quantitative proteomic analysis (table S4).

Capping the dynactin filament

The dynactin filament is similar to that of actin (24), consistent with the high (53%) sequence identity between β-actin and Arp1 (fig. S3B). Both consist of four subdomains surrounding a nucleotide binding site (fig. S4). A key contact within the filament is the subdomain-2 loop binding the groove between subdomains 1 and 3 on the neighboring subunit. Blocking this interaction provides a mechanism to cap both actin and dynactin filaments.

At the barbed end of dynactin a CapZαβ heterodimer binds across both protofilaments. The C-terminal helices (tentacles) of CapZα and CapZβ fit into the subdomain 1 and 3 groove on Arp1-B and Arp1-A (Fig. 2A, fig. S5 and movie S3) and prevent further subunit binding. CapZαβ interacts with dynactin in the same way as proposed for the actin filament (25). However, there is a loop (called the plug) (24) that contains four negatively charged residues in Arp1 but only one in actin (Fig. 2B). This loop is close to a cluster of four positively charged residues on CapZα suggesting CapZαβ binds Arp1 with a higher affinity than actin. This explains why a pool of CapZαβ remains bound to dynactin but not to actin, when most CapZαβ is depleted by siRNA (26). The tight binding of CapZαβ reflects its role in stabilizing dynactin's structure.

At the pointed end the bottom protofilament ends in β-actin whereas the top ends in Arp1 (Fig. 1A). This creates a distinctive binding site for Arp11, the most evolutionarily distant of all the actin related proteins (27). Our structural data reveal how a single Arp11 subunit can cap both protofilaments. The bottom protofilament directly binds Arp11 which prevents further subunit addition because its subdomain-2 loop is too short (27) (Fig. 2C). Subunit addition to the Arp1-I subunit on the top protofilament is blocked sterically by subdomain-4 of Arp11 (asterisk in Fig. 2D) and also because the Arp1-I subdomain-2 loop is sequestered by Arp11 (Fig. 2D).

Arp11 binds p25, p27 and p62 to form the pointed end complex (Fig. 2E). The p25 and p27 subunits consist of a triangular β-sheet structure (22) followed by an α-helix (fig. S6). They pack side to edge (fig. S6A) and bind end-on to Arp11 (Fig. 2F). The interaction is reinforced by p62 which wraps around the Arp11:p25-p27 contact site (Fig. 2E). Only Arp11 directly caps the pointed end, suggesting that the other components have a different role such as cargo attachment (28). Indeed, some fungal species contain Arp11 but lack p25, p27 and p62 (29).

The p150[Glued] projection extends over 50 nm from the shoulder

Previous antibody labeling showed p150[Glued] forms dynactin's shoulder projection (7). Existing models suggest it is 24 nm long and contains the p150[Glued] N-terminal Cap-Gly domain and CC1A coiled coil (Fig. 3A) (7, 8). The projection is not visible in our high-resolution EM maps owing to its flexibility. However, we determined an 8.6Å structure from a subset of particles (Fig. 3B, table S1 and fig. S7) in which it is visible because it docks against the side of dynactin (fig. S8A,B). The projection is over 50 nm long and contains three coiled coils, which we assigned to those in p150[Glued] based on their length (fig. S8C). An ~18 nm coiled coil (CC2) emerges from the shoulder and joins a globular domain consisting of a dimer (fig. S8D) of two ~40 kDa subunits (inter coiled domain: ICD). Another ~24 nm coiled coil (CC1B) extends from the ICD before doubling back for ~18 nm (CC1A). Our model predicts that the Cap-Gly domain at the N-terminus of CC1A is located close to the ICD. This is not visible in our structure owing to its flexibility and because the majority of our dynactin contains the shorter isoform of p150[Glued] (p135) which lacks a Cap-Gly domain (Fig. 3A). Our 50 nm projection is similar in appearance to structures observed in the images of dynactin viewed by rotary shadowing (7). Furthermore,

the interaction made by CC1A folding back onto CC1B agrees with recent biochemical data (30) and unpublished negative stain EM data (Y. Toyoshima, personal communication).

The shoulder's symmetry is broken by binding the dynactin filament

Previous models suggest the shoulder consists mainly of p150[Glued] (8). Our finding that most of p150[Glued] is in the projection implies the shoulder contains predominantly p24 and p50. We confirmed dynactin contains four copies of p50 and 2 copies of p24 (27) because the mass calculated from this stoichiometry matches (table S4) that measured by mass spectrometry (1,066,889 Da - Fig. 3C). We verified this composition by tandem MS (Fig. 3D) and measuring the resulting sub-complexes (table S5).

The shoulder's flexibility results in a lower resolution cryo-EM map and makes it challenging to assign individual α-helices to specific proteins. Instead the structures reveal an intrinsic two fold symmetry of the shoulder that was not obvious in previous images of dynactin (17). The shoulder contains two identical arms (Fig. 3E,F), made of bundles of three α-helices (Fig. 1D), which meet at a dimerization domain (fig. S9A). The end of each arm meets another short bundle of helices at an acute angle (hook domain) and a variably positioned paddle domain (Fig. 3E and fig. S9B). The symmetry between the two arms is broken as they twist to contact the dynactin filament.

The stoichiometry of p24 and p50, and their predicted helical and coiled coil structures (8, 31) suggest each arm contains one helix from p24 and two from p50. The length of p24 (186 residues) is similar to the length of the arm, whereas that of p50 (401 residues) is longer, suggesting p50 contributes to other structures such as the hook or paddle domain. The two p150[Glued] copies enter the shoulder between the two arms (Fig. 3F), split and run along each arm before joining the hook domains. Thus the role of the p150[Glued] C-terminus is to stick the two p50/p24 arms together.

Extended peptides from the shoulder span the length of the dynactin filament

The invariant size of the dynactin filament implies some mechanism specifies its length (7, 17, 32). The shoulder is the best candidate for dynactin's molecular ruler. Its main body contacts four Arp1 subunits close to the barbed end (fig. S10). In addition four extended regions (ERs) emerge from it and coat the rest of the filament (Fig. 4). The ends of all four are structurally identical (fig. S11A-D) suggesting they correspond to p50 which is the only tetramer in dynactin (8). The ERs are most likely the N-termini of p50, which are predicted to be unstructured, contain sequence that fits the clearest parts of the ER density (fig. S11E) and are able to displace the shoulder from the dynactin filament (26). Two pairs of ERs emerge from each shoulder paddle (Fig. 4A,B). One of each pair contacts the top protofilament: ER-1 runs from Arp1-C to Arp1-E and ER-2 from Arp1-G to Arp1-I (Fig. 4C). The other reaches down to contact the bottom protofilament: ER-3 runs from Arp1-B to Arp1-D and ER-4 contacts Arp1-F (Fig. 4D). The ends of all four ERs occupy a positively charged groove on the dynactin filament that is equivalent to the tropomyosin binding groove on actin (33) (fig. S12A,B). While structurally different from tropomyosin (24), the

N-terminus of p50 is similarly rich in negatively charged residues (fig. S12C) suggesting why both bind an equivalent site.

The shoulder and its ERs contact every filament subunit except for β-actin-H (fig. S12D), suggesting the following model for dynactin assembly. The shoulder and ERs recruit eight Arp1s and stabilize their polymerization into a structure with 5 subunits on the top protofilament and three on the bottom. The gap in position H is filled by β-actin perhaps owing to actin's high abundance in the cell. The unique interface formed by Arp1-I and β-actin-H specifically recruits Arp11. Together with CapZαβ binding to the barbed end this results in a highly stable complex of an exactly defined length.

Dynein and BICD bind the dynactin filament

Dynein, dynactin and the N-terminus of BICD2 (BICD2N) only form a stable complex when all three components are present (12-14). In this dynein-dynactin-BICD2N (DDB) complex dynein binds dynactin via its tail, while its motor domains remain flexible (13). Currently there are no 3D structures of either the dynein tail or its interaction with dynactin. We therefore formed a stable tail-dynactin-BICD2N (TDB) complex (fig. S13) and determined its structure by cryo-EM to 8.2Å (fig. S14 and movie S4).

The dynein tail binds directly to the Arp1 filament (Fig. 5A,B) stretching from β-actin-H to the barbed end. The interaction is stabilized by a ~270 residue coiled coil of BICD2N which runs the length of the filament. Projections of the TDB complex are very similar to negative stain images of the DDB complex (fig. S15) (13) suggesting that the flexible, C-terminal motor domains of dynein lie close to the barbed end of dynactin (fig. S15). To determine the orientation of BICD2N we removed the N-terminal GFP tag (table S1 and fig. S16) and showed that the globular density at one end disappeared (fig. S16). Therefore the BICD2N N-terminus lies close to the barbed end and its C-terminus emerges from the pointed end. The C-terminus of BICD2 and the pointed end complex of dynactin, which are implicated in cargo binding (28, 34), are thus diametrically opposed to the dynein motor domains (Fig. 5A).

The dynein heavy chain contains an N-terminal dimerization domain

The dynein tail consists of two copies of the dynein heavy chain (DHC), intermediate chain (DIC2), light intermediate chain (DLIC1) and light chains (Roadblock, Tctex and LC8). The tail, within the TDB complex, contains two elongated S-shaped domains corresponding to the DHCs: chain-1 and chain-2 (Fig. 5C). The DHC C-termini, which contain the binding site for DLIC1 (35), are mainly disordered (Fig. 5B). The middle of each DHC wraps around a circular density corresponding in size, shape and position (35) to the WD40 β-propeller of DIC2 (Fig. 5C and fig. S17). Towards their N-termini the two DHC chains are joined by a small (~40 kDa), globular domain (Fig. 5C). We hypothesized that this domain represents a previously unknown dimerization domain of the DHC itself. To verify this we determined a crystal structure of the N-terminal 557 amino acids of the *S.cerevisiae* DHC (Dyn1[1-557]) to 5Å resolution (Fig. 5D, fig. S18 and table S6). This shows two elongated domains, made up of bundles of α-helices, that fit well with the helices observed by cryo-

EM (fig. S18C,D). Furthermore it reveals that the elongated domains are joined by an N-terminal dimerization domain (Fig. 5D).

In the crystal structure the elongated domains are related by rotational symmetry with their C-termini pointing in opposite directions (Fig. 5D). In the TDB structure, each elongated domain has rotated about the flexible connection to the dimerization domain (movie S5) so that they lie parallel to each other (Fig. 5E). This is probably caused by the light chain mediated dimerization of DIC2 (36, 37) holding the DHCs together towards their C-termini.

The symmetry in the dynein tail matches the dynactin filament

The N-termini of the elongated domains have translational symmetry (a sideways movement relates one onto the other) (Fig. 5E) which matches that of their binding sites on the filament (Fig. 5F). They bind adjacent clefts between Arp1-D & F (chain-1) and Arp1-F & β-actin-H (chain-2) (Fig. 5F,G). These sites are equivalent to the myosin motor binding site on actin (fig. S19 and movie S6). The translational symmetry between DHC chains is lost towards their C-termini as chain-2 twists relative to chain-1 (Fig. 5C). Chain-2 makes no further contacts with the dynactin filament, whereas chain-1 binds it again at Arp1-A&C (Fig. 5H).

BICD2N is involved in all dynein-tail/dynactin-filament interactions (Fig. 5F,G,H and movie S7). In the Arp1-D/F and Arp1-F/β-actin-H clefts, BICD2N stabilizes the interaction of the DHC chains with the filament (Fig. 5G). At the Arp1-A&C site BICD2N sits between chain-1 and dynactin. The network of contacts from BICD2N to dynein, BICD2N to dynactin and dynein to dynactin explains why all three components must be present to form a stable complex (12-14). The long BICD2N coiled coil may be suited as a cargo adaptor because it spans the length of the dynactin filament. Many other dynein adaptors, including TRAK1&2 (38), RILP (39), Rab11-Fip3, Hook3 and Spindly (14) contain coiled coils and may recruit dynein and dynactin in a similar way. The requirement to form a three-way complex would reduce the chance of stochastic binding of dynein to its cargos.

The shoulder coats three sides of the filament (fig. S12B,C) leaving the front face free for interaction with BICD2N and the dynein tail. It does not, however, contact dynein in our structure. One well reported interaction between dynein and dynactin involves the p150[Glued] CC1 region and the N-terminus of DIC2 (11). Both regions are too flexible in our structure to be visualized directly. However the p150[Glued] projection binds to the same face of the dynactin filament as BICD2N (Fig. 3B and Fig. 5A,B) and both occupy the same cleft on the pointed end complex (fig. S8B and Fig. 5B). Thus BICD2N binding could free p150[Glued] CC1 to make contact with DIC2 and so add an additional contact that stabilizes the TDB complex.

How does recruitment of dynactin by a cargo adaptor (13, 14) activate dynein? Both the microtubule binding Cap-Gly (14) and DIC2 binding CC1B (30) regions of p150[Glued] have been implicated. Our structure raises a third, but not mutually exclusive, possibility. Studies with artificially dimerized dynein motor domains suggest they self-associate in an auto-inhibited conformation unless they are sufficiently separated (40). We suggest dynactin activates the motor domains by reorienting the two DHCs. Both DHC N-termini are anchored parallel to each other, but the C-termini are forced to twist apart because only one

chain binds the second site on dynactin. This hypothesis explains why dynactin is built around an actin-like filament. The translational symmetry of the filament matches that of the DHC N-termini, whereas the filament length provides additional binding sites that force dynein to adopt its active conformation.

Supplementary Material

Refer to Web version on PubMed Central for supplementary material.

Acknowledgments

References and Notes

1. Gill SR, et al. J. Cell Biol. 1991; 115:1639–1650. [PubMed: 1836789]

2. McGrail M, et al. J. Cell Biol. 1995; 131:411–425. [PubMed: 7593168]

3. Plamann M, Minke PF, Tinsley JH, Bruno KS. J. Cell Biol. 1994; 127:139–149. [PubMed: 7929559]

4. Allan VJ. Biochem. Soc. Trans. 2011; 39:1169–1178. [PubMed: 21936784]

5. Schiavo G, Greensmith L, Hafezparast M, Fisher EMC. Trends Neurosci. 2013; 36:641–651. [PubMed: 24035135]

6. Dodding MP, Way M. EMBO J. 2011; 30:3527–3539. [PubMed: 21878994]

7. Schafer DA, Gill SR, Cooper JA, Heuser JE, Schroer TA. J. Cell Biol. 1994; 126:403–412. [PubMed: 7518465]

8. Schroer TA. Annu Rev Cell Dev Biol. 2004; 20:759–779. [PubMed: 15473859]

9. Siglin AE, et al. PLoS ONE. 2013; 8:e59453. [PubMed: 23577064]

10. Duellberg C, et al. Nat. Cell Biol. 2014; 16:804–811. [PubMed: 24997520]

11. King SJ, Brown CL, Maier KC, Quintyne NJ, Schroer TA. Molecular Biology of the Cell. 2003; 14:5089–5097. [PubMed: 14565986]

12. Splinter D, et al. Molecular Biology of the Cell. 2012; 23:4226–4241. [PubMed: 22956769]

13. Schlager MA, Hoang HT, Urnavicius L, Bullock SL, Carter AP. EMBO J. 2014; 33:1855–1868. [PubMed: 24986880]

14. McKenney RJ, Huynh W, Tanenbaum ME, Bhabha G, Vale RD. Science. 2014; 345:337–341. [PubMed: 25035494]

15. Dienstbier M, Li X. Biochem. Soc. Trans. 2009; 37:1066–1071. [PubMed: 19754453]

16. Hodgkinson JL, Peters C, Kuznetsov SA, Steffen W. Proc Natl Acad Sci U S A. 2005; 102:3667–3672. [PubMed: 15738427]

17. Imai H, Narita A, Maéda Y, Schroer TA. J Mol Biol. 2014; 426:3262–3271. [PubMed: 25046383]

18. Bingham JB, Schroer TA. Curr. Biol. 1999; 9:223–226. [PubMed: 10074429]

19. Bai X-C, McMullan G, Scheres SHW. Trends Biochem. Sci. 2015; 40:49–57. [PubMed: 25544475]

20. Materials and methods are available as supplementary materials on Science Online.

21. Yamashita A, Maeda K, Maéda Y. EMBO J. 2003; 22:1529–1538. [PubMed: 12660160]

22. Yeh TY, et al. EMBO J. 2013; 32:1023–1035. [PubMed: 23455152]

23. Holleran EA, Tokito MK, Karki S, Holzbaur EL. J. Cell Biol. 1996; 135:1815–1829. [PubMed: 8991093]

24. von der Ecken J, et al. Nature. 2014 doi:10.1038/nature14033.

25. Narita A, Takeda S, Yamashita A, Maéda Y. EMBO J. 2006; 25:5626–5633. [PubMed: 17110933]

26. Cheong FKY, Feng L, Sarkeshik A, Yates JR, Schroer TA. Molecular Biology of the Cell. 2014; 25:2171–2180. [PubMed: 24829381]

27. Eckley DM, et al. J. Cell Biol. 1999; 147:307–320. [PubMed: 10525537]

28. Yeh TY, Quintyne NJ, Scipioni BR, Eckley DM, Schroer TA. Molecular Biology of the Cell. 2012; 23:3827–3837. [PubMed: 22918948]

29. Hammesfahr B, Kollmar M. BMC Evol. Biol. 2012; 12:95. [PubMed: 22726940]

30. Tripathy SK, et al. Nat. Cell Biol. 2014; 16:1192–1201. [PubMed: 25419851]

31. Pfister KK, Benashski SE, Dillman JF, Patel-King RS, King SM. Cell Motil. Cytoskeleton. 1998; 41:154–167. [PubMed: 9786090]

32. Lees-Miller JP, Helfman DM, Schroer TA. Nature. 1992; 359:244–246. [PubMed: 1528266]

33. Behrmann E, et al. Cell. 2012; 150:327–338. [PubMed: 22817895]

34. Liu Y, et al. Genes Dev. 2013; 27:1233–1246. [PubMed: 23723415]

35. Tynan SH, Gee MA, Vallee RB. J. Biol. Chem. 2000; 275:32769–32774. [PubMed: 10893223]

36. Williams JC, et al. Proc Natl Acad Sci U S A. 2007; 104:10028–10033. [PubMed: 17551010]

37. Benison G, Karplus PA, Barbar E. J Mol Biol. 2007; 371:457–468. [PubMed: 17570393]

38. van Spronsen M, et al. Neuron. 2013; 77:485–502. [PubMed: 23395375]

39. Jordens I, et al. Curr. Biol. 2001; 11:1680–1685. [PubMed: 11696325]

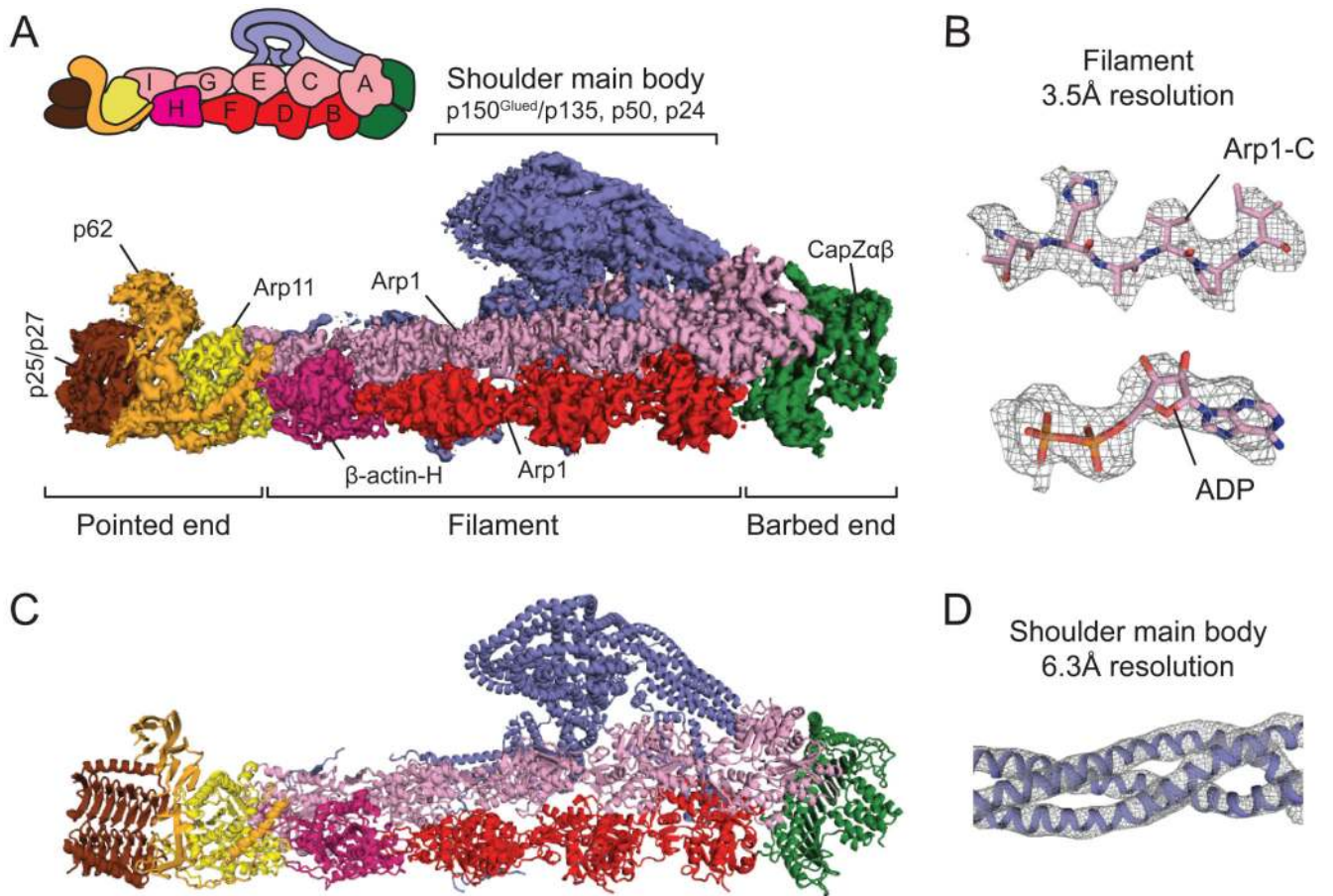40. Torisawa T, et al. Nat. Cell Biol. 2014; 16:1118–1124. [PubMed: 25266423]

Fig. 1. Cryo-EM structure of dynactin
(**A**) A 4.0Å cryo-EM map of dynactin segmented and colored according to its components.
(**B**) A density map of a β-strand and ADP molecule in Arp1-C. (**C**) A molecular model of
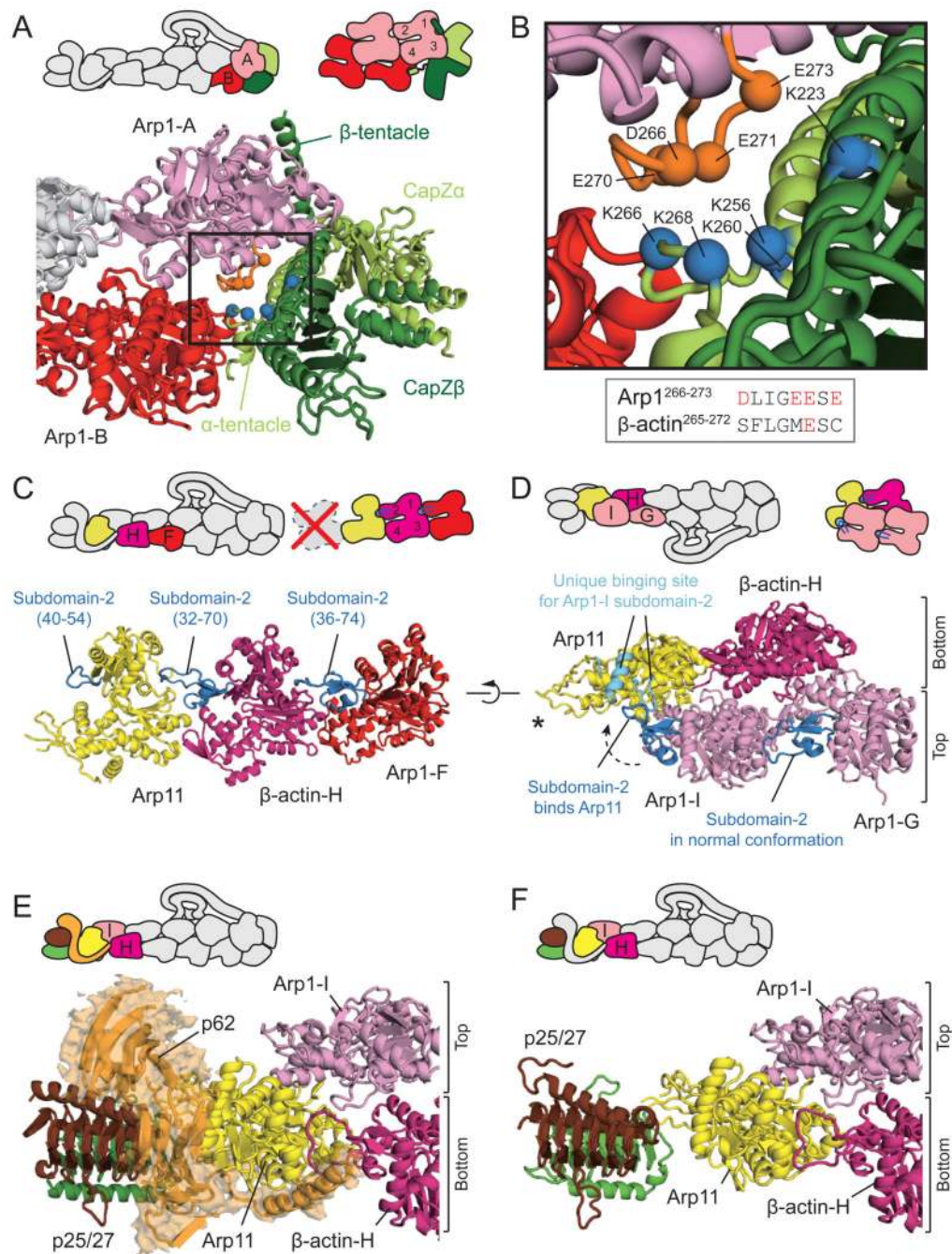dynactin. (**D**) 6.3Å cryo-EM map showing helices in the dynactin shoulder.

Fig. 2. Capping the dynactin filament

(**A**) The barbed end is capped by CapZαβ. (**B**) CapZαβ contains five positive residues (blue) which interact with four negative residues (orange) on Arp1. The equivalent loop in actin contains only one negative residue. (**C**) The short Arp11 subdomain-2 loop prevents further subunit addition to the bottom protofilament. (**D**) Arp11 caps the top protofilament by binding the subdomain-2 loop of Arp1-I and sterically blocking (asterisk) subsequent subunit binding. (**E**) The pointed end complex: p62 extends over Arp11 to touch β-actin-H. (**F**) p25 and p27 pack end-on to Arp11 as a continuation of the bottom protofilament.
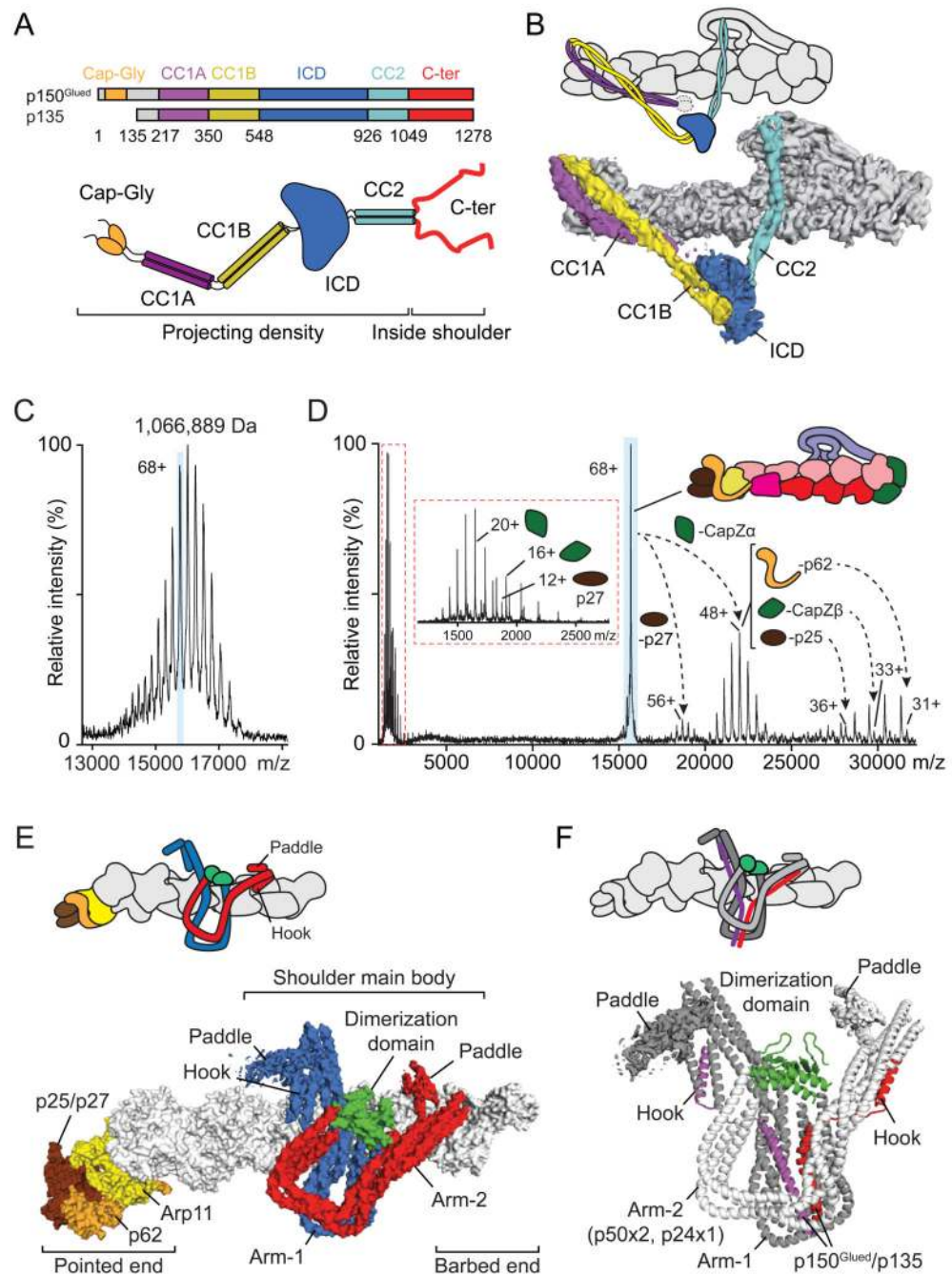
Fig. 3. The architecture of the p150^Glued projection and shoulder
(**A**) Schematic models of p150^Glued. (**B**) An 8.6Å cryo-EM structure with a docked p150^Glued projection, colored according to A. (**C**) Native mass spectrometry of dynactin reveals the mass of the intact complex. (**D**) Tandem MS confirms the subunit composition of the complex. (**E**) The shoulder contains two arms (red and blue) that emerge from a dimerization center (green) and end in hook and paddle domains. (**F**) The C-terminus of the p150^Glued dimer enters the shoulder and splits into separate helices.
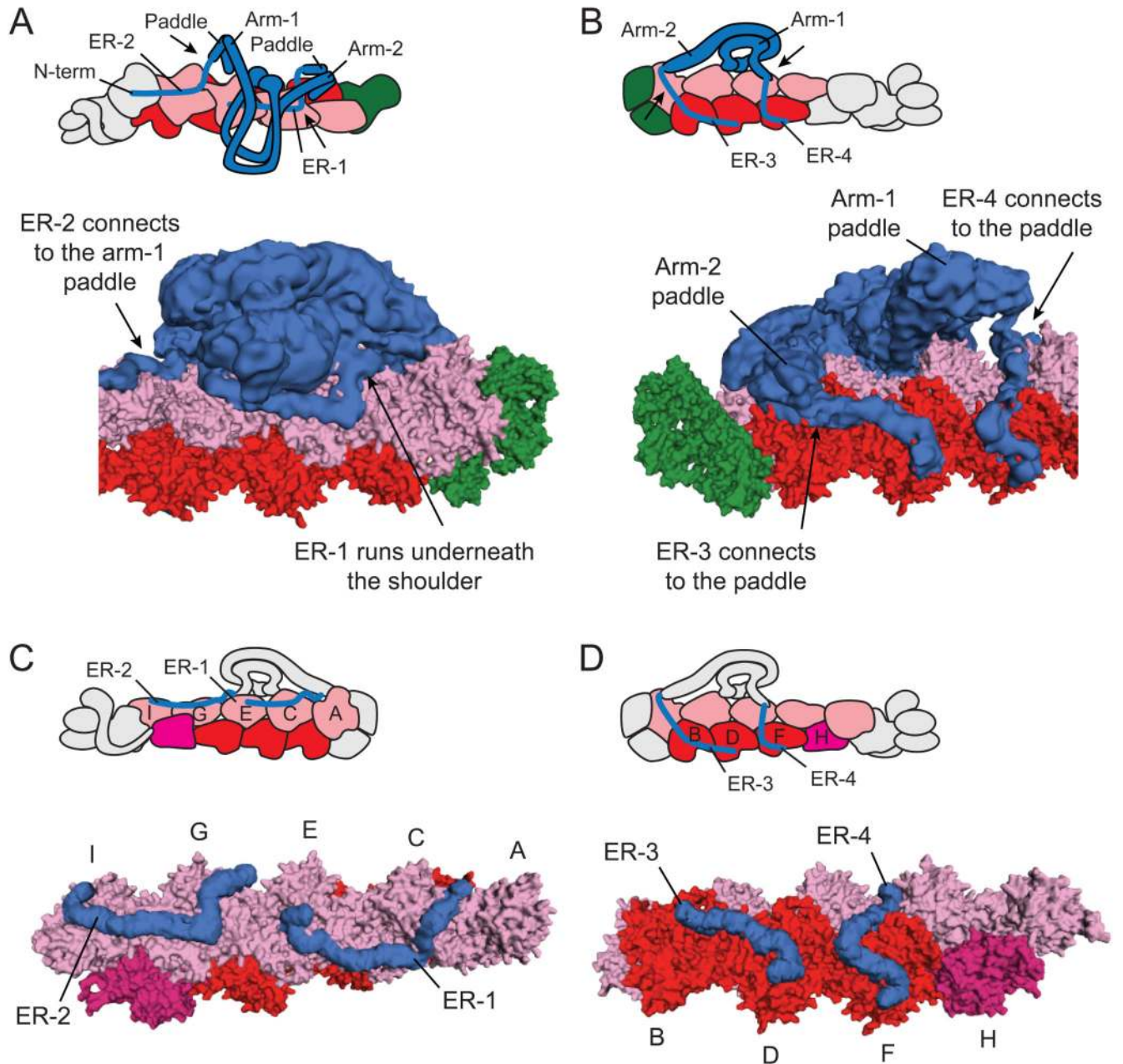
Fig. 4. Shoulder peptides coat and measure the dynactin filament

(**A,B**) Four extended regions (ER1-4) connect to the shoulder paddles. (**C**) ER1-2 cover the full length of the top Arp1 protofilament. (**D**) ER3-4 cover the bottom protofilament subunits Arp1-B,D&F, but not the β-actin-H subunit.
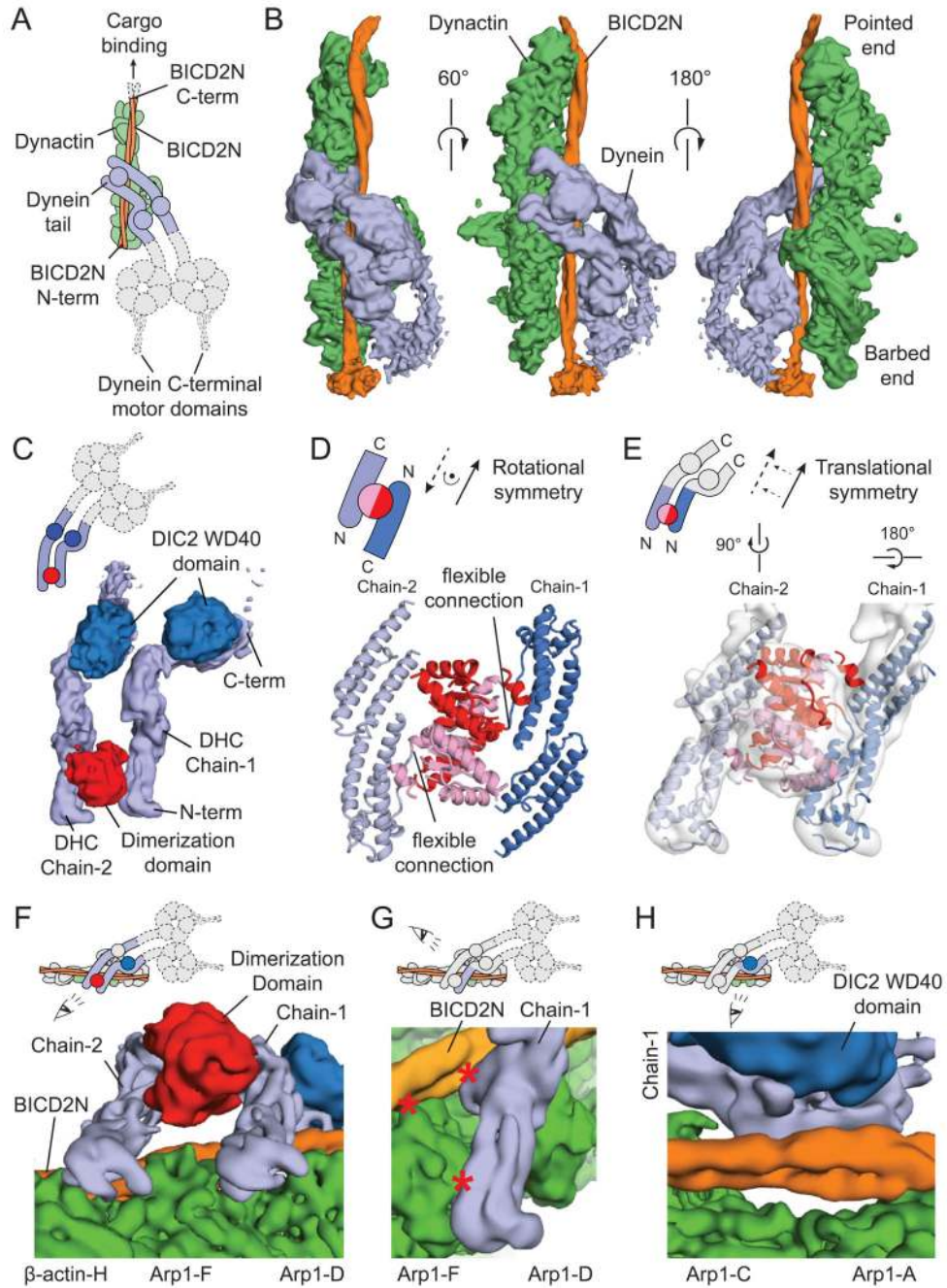
Fig. 5. The dynein tail and its interaction with dynactin and BICD2N

(**A**) Cartoon model of the dynein tail/dynactin/BICD2N complex (TDB). (**B**) An 8.2Å cryo-EM structure of TDB. (**C**) An N-terminal domain dimerizes the dynein heavy chain (DHC) elongated domains, which wrap round the dynein intermediate chain (DIC2). (**D**) Crystal structure of the *S.cerevisiae* DHC N-terminus (Dyn1[1-557]). (**E**) The Dyn1[1-557] structure fits well into the cryo-EM map. (**F**) The translational symmetry of DHC chain-1 and 2 matches

the dynactin filament. (**G**) Interaction of chain-1 with BICD2N and dynactin (asterisks). (**H**) The second interaction site of chain-1 with dynactin is solely mediated by BICD2N.